Morphometrical analysis of the canine choroid in relation to age and sex using spectral domain optical coherence tomography

JOWITA ZWOLSKA[1], MATEUSZ SZADKOWSKI[1]* ,
AGNIESZKA BALICKA[2] and IRENEUSZ BALICKI[1]

[1] Department and Clinic of Animal Surgery, Faculty of Veterinary Medicine, University of Life Sciences in Lublin, Akademicka 13, 20-950 Lublin, Poland

[2] Small Animal Clinic, University of Veterinary Medicine and Pharmacy in Košice, Košice, Slovakia

RESEARCH ARTICLE

Check for updates

ABSTRACT

This study determined the choroidal thickness of senior (SN, $n = 24$) and middle-aged (MA, $n = 17$) healthy, mixed-breed mesocephalic dogs, both males (M) and females (F), using spectral domain optical coherence tomography (SD-OCT). The dogs were divided into two groups for examination: MA dogs (4–7 years old; 6 M, 11 F) and SN dogs (8–13 years old; 12 M, 12 F). Choroidal thickness of the dogs was investigated using SD-OCT radial and linear scans. The software of the device allowed determination of the exact measurement location on the choroid. Measurements of the choroid were taken manually using the SD-OCT calliper function at distances of 5,000–6,000 μm (dorsal and ventral) and 4,000–7,000 μm (nasal and temporal) from the optic disc. Mean (μm ± SD) (MA, SN) dorsal (188 ± 28, 184 ± 33), ventral (116 ± 23, 111 ± 16), temporal (152 ± 31, 151 ± 26), and nasal (135 ± 27, 132 ± 18) choroidal thicknesses demonstrated significant differences ($P < 0.02$–0.001) between all areas within each group. The choroid was thickest in the dorsal region and thinnest in the ventral region. There were no significant differences based on age. Mean (μm ± SD) (M, F) dorsal (181 ± 32, 190 ± 30), ventral (117 ± 16, 11 ± 21), temporal (150 ± 26, 153 ± 30), and nasal (128 ± 20, 138 ± 23) choroidal thicknesses demonstrated significant differences ($P < 0.05$) between dorsal and nasal regions. The choroidal thickness in dogs depends on the area assessed independently of their age and sex.

INTRODUCTION

The structure, functional capacity, and biochemical reactions of the retina are sufficiently complex that a dual vascular supply is present in most species. The choroid is an anatomical structure located between the sclera and the retinal pigment epithelium (RPE) with the primary function of supplying oxygen and nutrients to the retina (Samuelson, 2013; McLellan and Narfstrom, 2014). Its coverage extends to almost the entire posterior half of the bulb of the eye. The choroid is primarily composed of blood vessels, nerves, and pigment cells.

The choroid supplies the adjacent retina layers that lack blood vessels. Oxygen and nutrients for the outer retina are transported through the RPE from the choriocapillaris of the choroid (Dubielzig et al., 2010). In other layers of the retina, blood perfusion is maintained by internal vessels originating from the short posterior ciliary arteries (therefore referred to as cilioretinal arteries). These vessels are usually visible on the surface of the fundus of the eye during an ophthalmoscopic examination (Ofri, 2018). Specifically, retinal blood vessels are found within the nerve fibre, ganglion cell, and inner plexiform layers of the inner retina. Capillaries are also present in the inner nuclear layer (Dubielzig et al., 2010). In addition to its

*Corresponding author. Tel.: +48 504 873 735.
E-mail: matszadkowski@gmail.com

nutritive function, the choroid also facilitates thermoregulation for maintaining the high metabolic activity of the retina.

In human medicine, a correlation has been observed between the choroid dimensions and patient characteristics such as age, sex, refractive error, axial length of the eye, corneal refractive power (Kim et al., 2011; Li et al., 2014; Shao et al., 2015; Zhu et al., 2017), and ethnic origin (Zhu et al., 2017). Higher hyperopic refractive error, lower age, being male, and higher corneal refractive power are examples of patient characteristics correlated with a greater choroidal thickness (Zhu et al., 2017). In a comparison of healthy children and adults, the greatest choroidal thickness was observed in the temporal region relative to the retinal macula of children, and the lowest in the nasal region. Adult choroidal thickness was the greatest in the fovea, followed by the temporal and the nasal regions (Ruiz-Moreno et al., 2013). The thickness of the choroid is also affected by the general clinical condition of the patient. Diseases that decrease plasma protein can result in reductions in oncotic pressure that cause increased choroidal thickness as a consequence of increased retina and choroid water retention. For instance, choroidal thickness was greater in paediatric patients with nephrotic syndrome than in controls (Zhang et al., 2019). Oncotic pressure reductions can also result in more serious conditions such as bilateral retinoschisis or macular oedema (De Benedetto et al., 2012).

Spectral domain optical coherence tomography (SD-OCT) is a non-invasive, non-contact method that provides real-time *in vivo* imagery of the retina (Murthy et al., 2016). This imagery of the posterior eye segment can document the emergence and development of various diseases. This method is also an objective method of measuring and analysing each retinal layer (Gabriele et al., 2011; McLellan and Rasmussen, 2012).

SD-OCT imaging of the canine choroid is a new research area. The choroid, being a multifunctional structure of the eye, can undergo pathological processes that may have a direct effect on visual function. The SD-OCT method is an ideal device for the *in vivo*, non-invasive imaging of choroidal morphology and morphometry. Recognition of the physiological image of the choroid in the SD-OCT scans will allow for further recognition of pathology. It may become an important diagnostic element.

The aim of this study was to determine choroidal thickness in senior (SN) and middle-aged (MA) mixed-breed mesocephalic dogs, both males (M) and females (F), using SD-OCT.

MATERIALS AND METHODS

Animals and procedures

Forty-one mixed-breed, mesocephalic, clinically healthy dogs were studied. The animals were patients of the Department and Clinic of Animal Surgery at the University of Life Sciences in Lublin. The owners were informed about the details of the clinical trials conducted and they gave their consent. The study was performed in accordance with the Polish law and with Directive 2010/63/EU of the European Parliament and of the Council of 22 September 2010 on the protection of animals used for scientific purposes, Chapter I, Article 1, point 5 (b). The research was also approved by the Scientific Research Committee of the Department and Clinic of Animal Surgery at the University of Life Sciences in Lublin (#3/2018) concerning non-experimental clinical patients.

The dogs were divided into two groups based on age. The classification was based on a dog age chart with regard to the relationship between age and weight (Fortney, 2012). Dogs in the MA group ($n = 17$; 6 M and 11 F) were 4–7 years old and weighed 12–34 kg. Dogs in the SN group ($n = 24$; 12 M and 12 F) were 8–13 years old and weighed 13–32 kg. All of the studied males were unneutered. The spay status of 4 females was unknown, while the remaining 19 females were non-spayed.

All dogs were classified as healthy based on physical examinations, complete ophthalmologic examinations, and blood test analyses. The blood tests included complete blood cell counts as well as the determination of urea, complete bilirubin, creatinine, aspartate transaminase, alanine transaminase, alkaline phosphatase, and amylase. The dogs had been dewormed twice a year.

Ocular examinations were performed using a slit lamp biomicroscope (Shin-Nippon, Japan). Fundus examinations were performed using a binocular indirect ophthalmoscope (Keeler, UK), a direct ophthalmoscope (Welch Allyn, USA), and a panoptic ophthalmoscope (Welch Allyn, USA). Photographs of the ocular fundus were taken using Handy NM-200D Fundus Camera (Nidek, Japan) connected to a computer operating IrfanView software (Wiener Neustadt, Austria). In all dogs, the pupillary light reflex, both direct and consensual, the dazzle reflex, the menace response, the palpebral reflex, and the corneal reflex were estimated. Behavioural ophthalmic tests that were conducted included tracking and placing or obstacle tests under scotopic and photopic conditions. Intraocular pressure (IOP) measurements were obtained using a rebound tonometer, TonoVet (iCare, Finland). The IOP in the study animals was 15–20 mmHg. Schirmer's Tear Test (Eickemeyer, Germany) was performed bilaterally over 60 s in all patients. No vision impairment or ocular abnormalities were identified in any dogs.

Sedation was provided with a use of medetomidine (0.03 mg kg^{-1}; Cepetor 1 mg mL^{-1}, CP Pharma, Germany) administered i.m. Local anaesthesia of the corneal and conjunctival surface was achieved using 0.5% proxymetacaine (Alcaine 5 mg mL^{-1}, Alcon, Poland). Pupils were dilated with tropicamide eye drops (Tropicamidum WZF 1%, Polfa Warszawa S.A., Poland). A timeframe was set for the OCT examination from 9 a.m. to 1 p.m. The examination was performed within 15–30 min after medetomidine administration. A thumb forceps was used to grasp the bulbar conjunctiva and to stabilise the eye.

OCT scan and data analysis

The examination was performed using SD-OCT (wavelength: 840 nm; scan pattern: enhanced depth imaging; Topcon 3D OCT-2000, Topcon, Japan) linear and 6-line radial scans. The device's software allowed determination of the precise location of choroidal measurements on the resulting scans. A calliper function integrated into the OCT software was used to collect manual measurements of the choroid. Choroidal thickness was defined as the vertical distance from the hyper-reflective line of the RPE–Bruch's membrane complex to the hyper-reflective line of the inner surface of the sclera. Measurements on linear scans were performed at distances of 5,000–6,000 μm (dorsal and ventral) and 4,000–7,000 μm (nasal and temporal) from the optic disc and were parallel to the horizontal diameter of the optic disc. Temporal and nasal scans were performed at the middle 1/3 height of the vertical diameter of the optic disc. Three measurements were conducted for each analysed segment: the first one in the centre of the scan and the other

two on the right and left at a distance of 1,500 μm from the centre (Figs 1 and 2). The central measurement on the scans of dorsal and ventral regions was taken on the width of the optic disc. The average of three measurements for each segment was calculated. The measurements were performed on 82 eyes of 41 dogs. During the SD-OCT examination, the cornea was moistened every 30 s with saline.

Statistical methods

Data normality was tested using the Shapiro–Wilk test. The results reported for the MA group followed a non-normal distribution, while results reported for the SN group followed a normal distribution. Data obtained from the ventral and nasal regions in females, and data from the nasal region in males followed a non-normal distribution. Significantly different comparisons were identified using the Mann–Whitney U test. Analyses were performed using Statistica 12 (TIBCO Software Inc., USA). A P value of <0.05 was considered statistically significant.
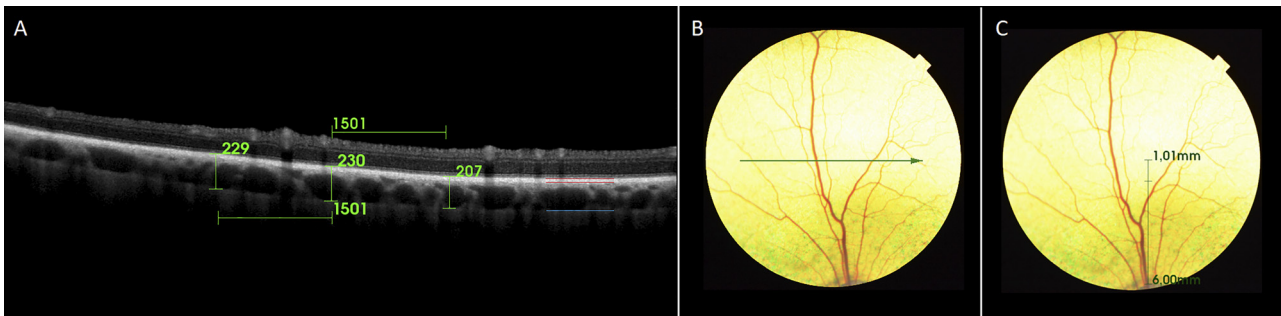

Fig. 1. A. Measurements of choroidal thickness in the dorsal region on a spectral domain optical coherence tomography (SD-OCT) scan. Three measurements were conducted for each analysed segment: the first one in the centre of the scan and the other two on the right and left at q distance of 1,500 μm from the centre. The red lines represent the borders of the retinal pigment epithelium (RPE)–Bruch's membrane– choriocapillaris and tapetum lucidum complex. The blue line represents the inner surface of the sclera. B. The location of the scan shown in Fig. 1A. C. Determination of the measurement site between 5,000 and 6,000 μm (distance from the optic disc). The scan was performed on a 1,000-μm segment visible as a short segment in the upper part of the determination
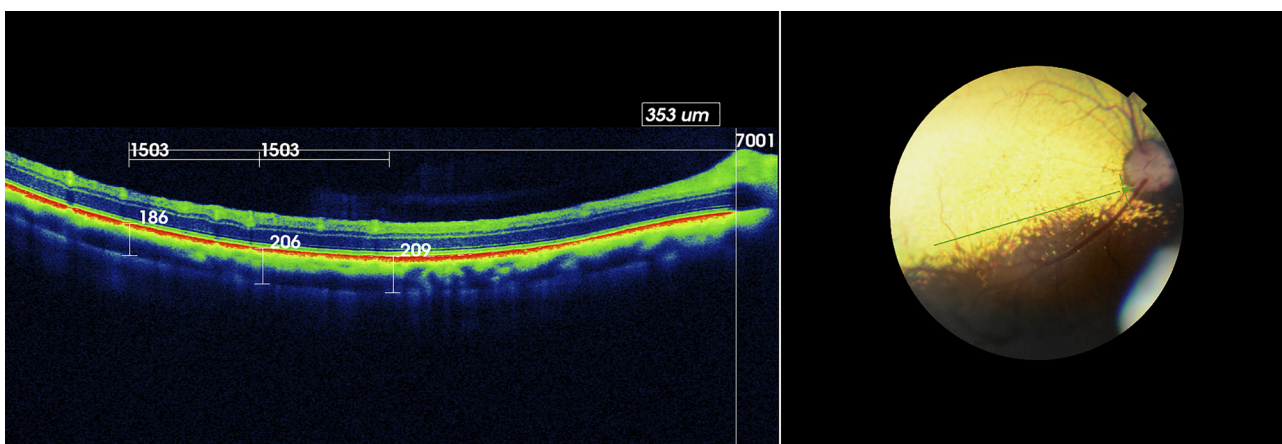

Fig. 2. Choroidal thickness measurements on an SD-OCT scan of the temporal region of the choroid. Three measurements were conducted for each analysed segment: the first one in the centre of the scan and the other two on the right and left at a distance of 1,500 μm from the centre. Measurements on linear scans were performed at distances of 4,000–7,000 μm (temporal and nasal). Temporal and nasal scans were performed at the middle 1/3 height of the vertical diameter of the optic disc

RESULTS

Thicknesses of the dorsal, ventral, temporal, and nasal regions of the choroid in the senior and middle-aged mixed-breed dogs are presented in Table 1. The dorsal choroid region was the thickest in both senior and middle-aged mixed breed mesocephalic dogs, the next thickest in the temporal region, and the thinnest in the ventral region. There was no statistically significant difference in the choroidal thickness of any of the four regions between the groups ($P > 0.05$) (Figs 3 and 4).

No significant, age-related discrepancies were observed in the thickness of the respective choroidal regions. However, statistically significant differences were observed between the respective choroidal regions within both the MA and the SN groups (Figs 3 and 4).

In the MA and SN group, choroidal thickness was significantly higher in the dorsal region than in the temporal ($P < 0.001$), nasal ($P < 0.001$) and ventral ($P < 0.001$) regions. The choroid in the temporal region was significantly thicker than in the nasal (MA, $P = 0.02$; SN, $P < 0.001$) and ventral

(MA, $P < 0.005$; SN, $P < 0.001$) regions. The choroid in the ventral region was significantly thinner than in the nasal region ($P < 0.001$) in both MA and SN groups.

Thicknesses of the dorsal, ventral, temporal, and nasal regions of the choroid in males and females are presented in Fig. 5 and Table 2. The dorsal choroid region was the thickest in both males and females, the next thickest in the temporal region, and the thinnest in the ventral region. Although no statistically significant difference was observed between dogs of different age groups, statistical differences were noted between males and females. The choroidal thickness was significantly greater in males than in females in the ventral region ($P < 0.005$). It was significantly thinner in males than in females in the nasal region ($P < 0.005$).

DISCUSSION

The aim of the study was to determine *in vivo* choroidal thickness in mixed-breed mesocephalic dogs by the use of SD-OCT. The location of the RPE–Bruch's membrane

Table 1. Mean choroidal thickness [µm] ± standard deviation (SD) reported for dorsal (D), ventral (V), temporal (T) and nasal (N) regions in the middle-aged (MA) and senior (SN) groups

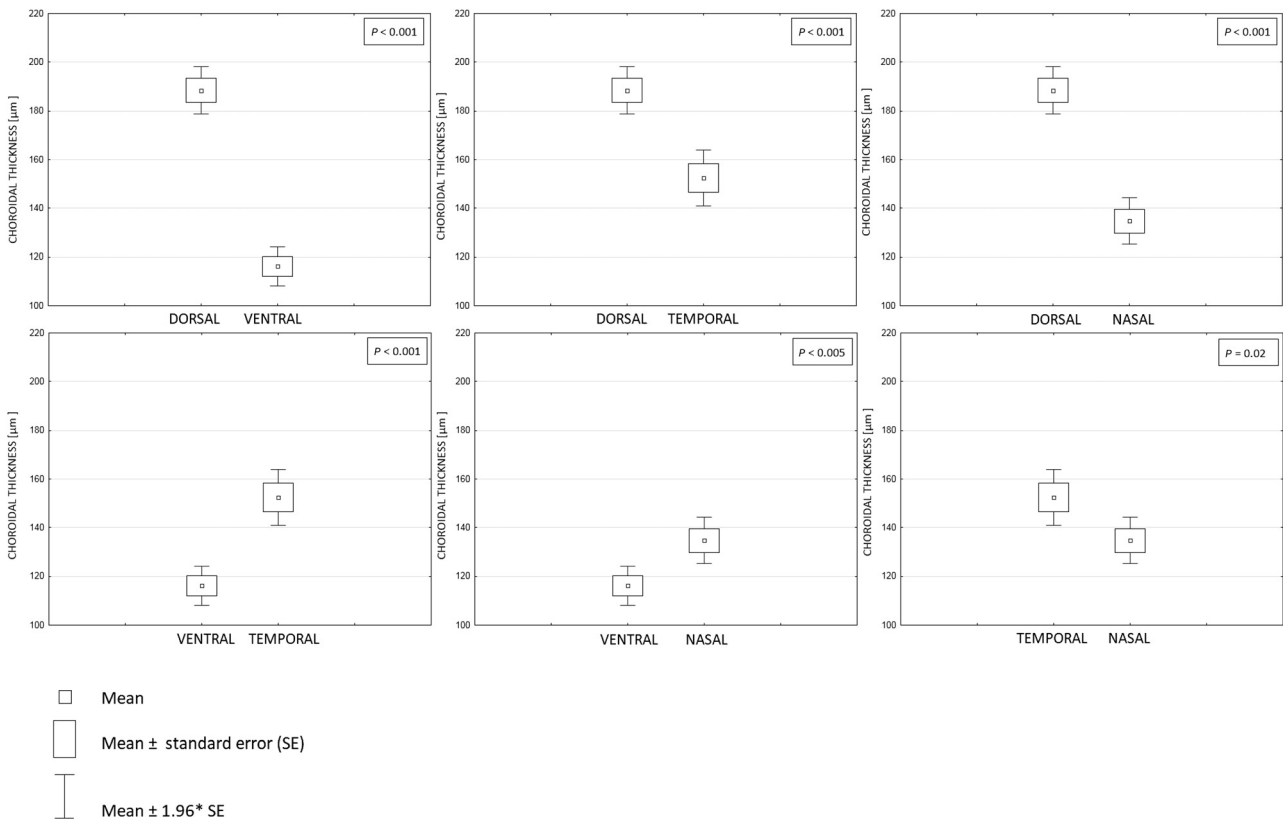|	D	V	T	N
MA	188 ± 28	116 ± 23	152 ± 30	135 ± 27
SN	184 ± 33	111 ± 16	151 ± 26	132 ± 18

Fig. 3. Comparison of the mean thickness and SE for each choroidal region in the middle-aged (MA) group
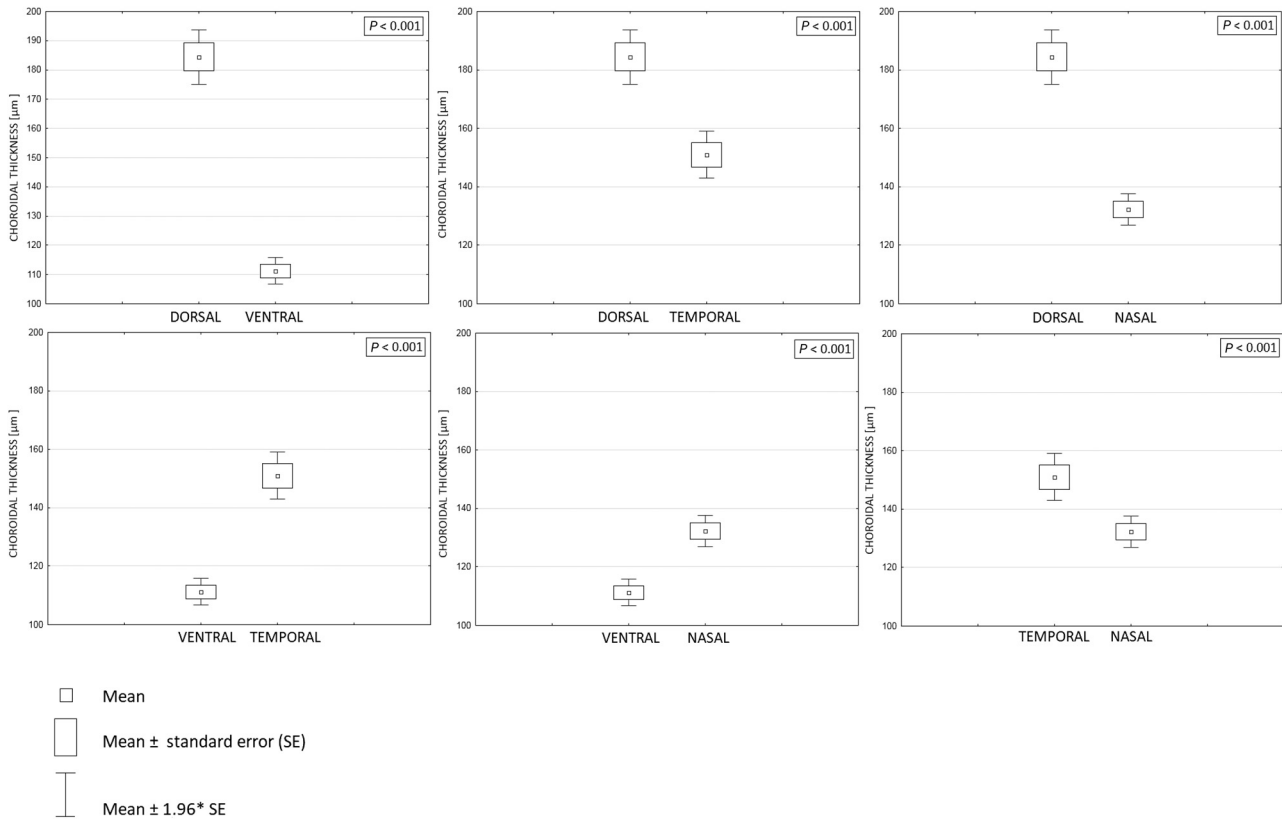
Fig. 4. Comparison of the mean thickness and SE for each choroidal region in the senior (SN) group
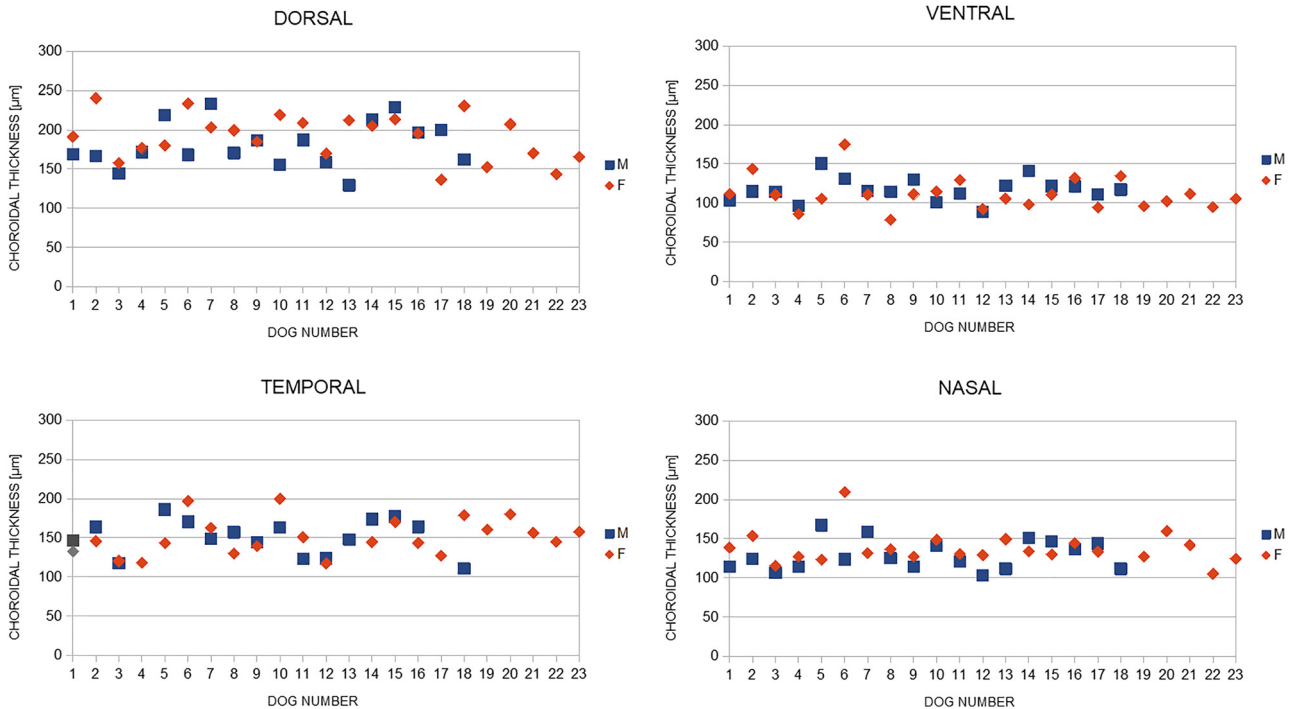

Fig. 5. Choroidal thicknesses reported for dorsal, ventral, temporal and nasal regions in males (M) and females (F)

complex and the inner scleral surface was determined by the human choroidal thickness measurement method (Jin et al., 2016; Abadia et al., 2018; Sahinoglu-Keskek and Canan, 2018; Steiner et al., 2019; Uyar et al., 2019; Pinheiro-Costa et al., 2020; Zhao et al., 2020), as well as on the basis of previous research on canine choroidal histology (Kotb et al.,

Table 2. Mean choroidal thickness [μm] ± standard deviation (SD) reported for dorsal (D), ventral (V), temporal (T) and nasal (N) regions in males (M) and females (F)

	D	V	T	N
M	181 ± 32	117 ± 16 [*]	150 ± 26	128 ± 20[*]
F	190 ± 30	111 ± 21	153 ± 30	138 ± 23

[*]Statistically significant difference between males and females ($P < 0.005$).

2019) and SD-OCT retinal imaging (Staurenghi et al., 2014; Carpenter et al., 2018; Grozdanic et al., 2019; Osinchuk et al., 2019; Graham et al., 2020; Occelli et al., 2020).

This study documented statistically significant differences between the respective choroidal regions within both the MA and the SN groups. The canine choroid is the thickest in the dorsal region, followed by the temporal and nasal regions, respectively, and it is the thinnest in the ventral region. Differences in choroidal thickness in the respective regions are related to the presence of the tapetum lucidum in the dorsal part of the choroid. The tapetum is described as rounded triangular with a smooth contour. Its base usually has contact with the optic nerve disc (Yamaue et al., 2014). The central part of the canine tapetum lucidum contains a light-reflecting material and consists of 15–20 layers of polygonal, zinc-rich cells with a mean thickness of 3–28 μm (Lesiuk and Breakevelt, 1983). The number of cell layers decreases with increasing distance from the centre of the tapetum. Bruch's membrane also varies in thickness and is thinnest in areas containing the tapetum lucidum (Lesiuk and Breakevelt, 1983). Yamaue et al. (2014) found that the thickest part of the tapetum was located dorso-temporally to the optic disk, varying in thickness from 20 to 70 μm. Such anatomical conditions have a direct impact on choroidal thickness when measured by SD-OCT. Yamaue et al. (2014) studied the canine tapetum in terms of its macroscopic variations and provided a histologic description of the macroscopic results. According to the study, the tapetum tended to be atypical with increasing age. The atypical tapetum was described to be smaller and more variable in shape, contour and colour than the typical one. The atypical tapetum had a tendency to disappear from the periphery, especially from the nasal and ventral parts. However, our study documented no significant age-related differences of the whole choroidal thickness when comparing the different regions. Therefore, individual layers of the canine choroid should be assessed in further studies.

This study reported statistically significant differences between males and females in dorsal and nasal choroidal regions. Sex discrepancies have been well documented in choroidal thickness measured by OCT in humans. Wang et al. (2018) found that men had a thicker choroid than women. Sanchez-Cano et al. (2014) found similar choroidal thickness for both males and females. Sex-related differences in choroidal thickness may be partially explained by the dissimilarity in sex hormone status. Oestrogen could affect ocular blood flow in females (Centofanti et al., 2000; Deschenes et al., 2010). This may influence choroidal thickness. The limitation of our study was the lack of data on the pregnancy status, oestrous cycle and hormonal treatment, and the absence of information about spaying/neutering performed on the dogs. If a study is restricted to humans, lifestyle practices inaccessible to most animals, such as smoking, alcohol consumption, caffeine intake, and exercise, may be unbalanced between the sexes. Such differences between individual women and men might be improperly attributed to sex. Nutritional status, medication intake, occupational factors, and even educational levels may also contribute to sex discrepancies in choroidal thickness (Wang et al., 2018).

A previous report used histomorphometric analyses to measure the choroidal thickness of five eyeballs acquired from adult, clinically healthy dogs (Kotb et al., 2019). However, these measurements were conducted post mortem. In contrast, we used SD-OCT to measure choroidal thickness *in vivo*. We documented that *in vivo* choroidal thickness is substantially greater than the 49.81 μm mean postmortem choroidal thickness previously reported for dogs.

Due to the possible impact of systemic diseases on our results, only data from clinically healthy animals were used in our study. We established the health status of dogs by clinical examinations that included complete blood count and biochemical blood test results that were within the reference ranges. We also conducted comprehensive ophthalmological examinations that documented the absence of ocular diseases that could affect our results.

Choroidal thickness cyclically varies throughout the day in chickens and humans (Nickla et al., 1998; Chakraborty et al., 2011). In chickens, choroidal thickness is the greatest at midnight, then it starts to decrease later during the night (Nickla et al., 1998). As in chickens, choroidal thickness increases also in humans over the course of the day, based on measurements taken between 9 a.m. and 9 p.m. To minimise the potential for diurnal variations in choroidal thickness, all measurements were taken between 9 a.m. and 1 p.m. This timeframe was determined based on reports which demonstrated that changes in choroidal thickness were minimal during those hours and varied no more than 3 μm. In contrast, the mean daily amplitude of change in choroidal thickness in humans was 0.029 ± 0.016 mm (Chakraborty et al., 2011).

Study conditions can potentially affect choroidal thickness. We are unaware of documentation of the impact of anaesthetics on choroidal thickness and cannot assess the degree to which these agents affected our results. However, it is known that anaesthetics can affect intraocular pressure (Webb et al., 2018) and there is a correlation between IOP

and choroidal thickness (Saeedi et al., 2014; Wang et al., 2016). To minimise the potential for IOP to affect our measurements of choroidal thickness, we only report data from dogs with IOPs of 15–20 mmHg. Previous research indicated that there were no significant changes of IOP in dogs at 5, 10, 20 and 40 min after medetomidine administration (Verbruggen et al., 2000; Kanda et al., 2015). We used sedation as this was the only means to perform high-quality scans positioned at the exact pre-determined distance from the optic nerve disc in all animals used in this study. In clinical practice, the authors normally perform OCT examinations of placid dogs under local anaesthesia or rarely after sedation.

In research on the sedative and cardiorespiratory effects of intramuscularly administered sedatives, medetomidine administration led to increased mean arterial blood pressure in dogs, compared with baseline values, up to 40 min from the time of administration. The highest increase occurred right after administration up to 10 min. Afterwards, arterial blood pressure remained increased following atipamezole administration (Ko et al., 2000). Therefore, we employed the same sedation protocol in all dogs to eliminate the possibility of anaesthesia-induced variation that could confound the choroidal thickness comparisons. The examination was conducted in the period between 15 and 30 min after medetomidine administration.

The aim of this research was to determine choroidal thickness in senior and middle-aged mixed-breed mesocephalic dogs, both males and females. The authors did not narrow the research to a particular dog breed. There are many ocular diseases that are diagnosed in mixed-breed dogs, e.g. Sudden Required Retinal Degeneration Syndrome (SARDS) is a disease often diagnosed in mixed-breed dogs (Heller et al., 2017). The authors chose this group of dogs due to the fact that many of the corresponding cases of mixed-breed dogs are being observed with various retinal and choroidal diseases. This group of patients might be a reference point for further studies regarding purebred dogs.

ACKNOWLEDGEMENTS

REFERENCES

Abadia, B., Suñen, I., Calvo, P., Bartol, F., Verdes, G. and Ferreras, A. (2018): Choroidal thickness measured using swept-source optical coherence tomography is reduced in patients with type 2 diabetes. PLoS One 13, e0191977.

Carpenter, C. L., Kim, A. Y. and Kashani, A. H. (2018): Normative retinal thicknesses in common animal models of eye disease using spectral domain optical coherence tomography. Adv. Exp. Med. Biol. 1074, 157–166.

Centofanti, M., Bonini, S., Manni, G., Guinetti-Neuschüler, C., Bucci, M. G. and Harris, A. (2000): Do sex and hormonal status influence choroidal circulation? Br. J. Ophthalmol. 84, 786–787.

Chakraborty, R., Read, S. A. and Collins, M. J. (2011): Diurnal variations in axial length, choroidal thickness, intraocular pressure, and ocular biometrics. Invest. Ophthalmol. Vis. Sci. 52, 5121–5129.

De Benedetto, U., Pastore, M. R., Battaglia Parodi, M., Bandello, F. and Pierro, L. (2012): Retinal involvement in nephrotic syndrome secondary to minimal change disease. Eur. J. Ophthalmol. 5, 843–845.

Deschenes, M. C., Descovich, D., Moreau, M., Granger, L., Kuchel, G. A., Mikkola, T. S., Fick, G. H., Chemtob, S., Vaucher, E. and Lesk, M. R. (2010): Postmenopausal hormone therapy increases retinal blood flow and protects the retinal nerve fiber layer. Invest. Ophthalmol. Vis. Sci. 51, 2587–2600.

Dubielzig, R. R., Ketring, K. L., McLellan, G. J., Albert, D. M. and Davis, F. A. (2010): The retina. In: Veterinary Ocular Pathology: A Comparative Review. Elsevier Saunders, Edinburgh. pp. 351–353.

Fortney, W. D. (2012): Implementing a successful senior/geriatric health care program for veterinarians, veterinary technicians, and office managers. Vet. Clin. North Am. Small. Anim. Pract. 42, 823–834.

Gabriele, M. L., Wollstein, G., Ishikawa, H., Kagemann, L., Xu, J., Folio, L. S. and Schuman, J. S. (2011): Optical coherence tomography: history, current status and laboratory work. Invest. Ophthalmol. Vis. Sci. 52, 2425–2436.

Graham, K. L., McCowan, C. I., Caruso, K., Billson, F. M., Whittaker, C. J. G. and White, A. (2020): Optical coherence tomography of the retina, nerve fiber layer, and optic nerve head in dogs with glaucoma. Vet. Ophthalmol. 23, 97–112.

Grozdanic, S. D., Lazic, T., Kecova, H., Mohan, K. and Kuehn, M. H. (2019): Optical coherence tomography and molecular analysis of sudden acquired retinal degeneration syndrome (SARDS) eyes suggests the immune-mediated nature of retinal damage. Vet. Ophthalmol. 22, 305–327.

Heller, A. R., van der Woerdt, A., Gaarder, J. E., Sapienza, J. S., Hernandez-Merino, E., Abrams, K., Church, M. L. and La Croix, N. (2017): Sudden acquired retinal degeneration in dogs: breed distribution of 495 canines. Vet. Ophthalmol. 20, 103–106.

Jin, P., Zou, H., Zhu, J., Xu, X., Jin, J., Chang, T. C., Lu, L., Yuan, H., Sun, S., Yan, B., He, J., Wang, M. and He, X. (2016): Choroidal and retinal thickness in children with different refractive status measured by swept-source optical coherence tomography. Am. J. Ophthalmol. 168, 164–176.

Kanda, T., Iguchi, A., Yoshioka, C., Nomura, H., Higashi, K., Kaya, M., Yamamoto, R., Kuramoto, T. and Furukawa, T. (2015): Effects of medetomidine and xylazine on intraocular pressure and pupil size in healthy Beagle dogs. Vet. Anaesth. Analg. 42, 623–628.

Kim, S.-W., Oh, J., Kwon, S.-S.,Yoo, J. and Huh, K. (2011): Comparison of choroidal thickness among patients with healthy eyes, early age-related maculopathy, neovascular age-related

macular degeneration, central serous chorioretinopathy, and polypoidal choroidal vasculopathy. Retina **9**, 1904–1911.

Ko, J. C., Fox, S. M. and Mandsager, R. E. (2000): Sedative and cardiorespiratory effects of medetomidine, medetomidine-butorphanol, and medetomidine-ketamine in dogs. J. Am. Vet. Med. Assoc. **216**, 1578–1583.

Kotb, A. M., Ibrahim, I. A. A., Aly, K. H. and Zayed, A. E. (2019): Histomorphometric analysis of the choroid of donkeys, buffalos, camels and dogs. Int. Ophthalmol. **39**, 1239–1247.

Lesiuk, T. P. and Breakevelt, C. R. (1983): Fine structure of the canine tapetum lucidum. J. Anat. **136**, 157–164.

Li, X. Q., Jeppesen, P., Larsen, M. and Munch, I. C. (2014): Subfoveal choroidal thickness in 1323 children aged 11 to 12 years and association with puberty: the Copenhagen Child Cohort 2000 Eye Study. Invest. Ophthalmol. Vis. Sci. **55**, 550–555.

McLellan, G. J. and Narfstrom, K. (2014): The fundus. In: Gould, D. and McLellan, G. (eds) Manual of Canine and Feline Ophthalmology. BSAVA, Quedgeley. pp. 322–356.

McLellan, G. J. and Rasmussen, C. A. (2012): Optical coherence tomography for the evaluation of retinal and optic nerve morphology in animal subjects: practical considerations. Vet. Ophthalmol. **15**, 13–28.

Murthy, R. K., Haji, S., Sambhav, K., Grover, S. and Chalam, K. V. (2016): Clinical applications of spectral domain optical coherence tomography in retinal diseases. Biomed. J. **39**, 107–120.

Nickla, D. L., Wildsoet, C. and Wallman, J. (1998): Visual influences on diurnal rhythms in ocular length and choroidal thickness in chick eyes. Exp. Eye Res. **66**, 163–181.

Occelli, L. M., Pasmanter, N., Ayoub, E. E. and Petersen-Jones, S. M. (2020): Changes in retinal layer thickness with maturation in the dog: an *in vivo* spectral domain–optical coherence tomography imaging study. BMC Vet. Res. **16**, 225.

Ofri, R. (2018): Diseases of the retina. In: Maggs, D., Miller, P. and Ofri, R. (eds) Slatter's Fundamentals of Veterinary Ophthalmology. Elsevier Saunders, Philadelphia. pp. 347–389.

Osinchuk, S. C., Leis, M. L., Salpeter, E. M., Sandmeyer, L. S. and Grahn, B. H. (2019): Evaluation of retinal morphology of canine sudden acquired retinal degeneration syndrome using optical coherence tomography and fluorescein angiography. Vet. Ophthalmol. **22**, 398–406.

Pinheiro-Costa, J., Correia, P. J., Pinto, J. V., Alves, H., Torrão, L., Moreira, R., Falcão, M., Carneiro, Â., Madeira, M. D. and Falcão-Reis, F. (2020): Increased choroidal thickness is not a disease progression marker in keratoconus. Sci. Rep. **10**, 19938.

Ruiz-Moreno, J. M., Flores-Moreno, I., Lugo, F., Ruiz-Medrano, J., Montero, J. A. and Akiba, M. (2013): Macular choroidal thickness in normal pediatric population measured by swept-source optical coherence tomography. Invest. Ophthalmol. Vis. Sci. **54**, 353–359.

Saeedi, O., Pillar, A., Jefferys, J., Arora, K., Friedman, D. and Quigley, H. (2014): Change in choroidal thickness and axial length with change in intraocular pressure after trabeculectomy. Br. J. Ophthalmol. **98**, 976–979.

Sahinoglu-Keskek, N. and Canan, H. (2018): Effect of latanoprost on choroidal thickness. J. Glaucoma **27**, 635–637.

Samuelson, D. A. (2013): Ophthalmic anatomy. In: Gelatt, K. N., Gilger, B. B. and Kern, T. J. (eds) Veterinary Ophthalmology. John Wiley & Sons, New York City. pp. 106–114.

Sanchez-Cano, A., Orduna, E., Segura, F., Lopez, C., Cuenca, N., Abecia, E. and Pinilla, I. (2014): Choroidal thickness and volume in healthy young white adults and the relationships between them and axial length, ammetropy and sex. Am. J. Ophthalmol. **158**, 574–583.

Shao, L., Xu, L., Zhang, J. S., You, Q. S., Chen, C. X., Wang, Y. X., Jonas, J. B. and Wei, W. B. (2015): Subfoveal choroidal thickness and cataract: The Beijing Eye Study 2011. Invest. Ophthalmol. Vis. Sci. **56**, 810–815.

Staurenghi, G., Sadda, S., Chakravarthy, U. and Spaide, R. F. (2014): International Nomenclature for Optical Coherence Tomography (IN•OCT) Panel. Proposed lexicon for anatomic landmarks in normal posterior segment spectral-domain optical coherence tomography: the IN•OCT consensus. Ophthalmology **121**, 1572–1578.

Steiner, M., Esteban-Ortega, M. D. M. and Muñoz-Fernández, S. (2019): Choroidal and retinal thickness in systemic autoimmune and inflammatory diseases: A review. Surv. Ophthalmol. **64**, 757–769.

Uyar, E., Dogan, U., Ulas, F. and Celebi, S. (2019): Effect of fasting on choroidal thickness and its diurnal variation. Curr. Eye Res. **44**, 695–700.

Verbruggen, A. M., Akkerdaas, L. C., Hellebrekers, L. J. and Stades, F. C. (2000): The effect of intravenous medetomidine on pupil size and intraocular pressure in normotensive dogs. Vet. Q. **22**, 179–180.

Wang, W., He, M. and Zhong, X. (2018): Sex-dependent choroidal thickness differences in healthy adults: A study based on original and synthesized data. Curr. Eye Res. **43**, 796–803.

Wang, Y. X., Jiang, R., Ren, X. L., Chen, J. D., Shi, H. L., Xu, L., Wei, W. B. and Jonas, J. B. (2016): Intraocular pressure elevation and choroidal thinning. Br. J. Ophthalmol. **100**, 1676–1681.

Webb, T. R., Wyman, M., Smith, J. A., Ueyama, Y. and Muir, W. W. (2018): Effects of propofol on intraocular pressure in premedicated and nonpremedicated dogs with and without glaucoma. J. Am. Vet. Med. Assoc. **257**, 823–829.

Yamaue, Y., Hosaka, Y. Z. and Uehara, M. (2014): Macroscopic and histological variations in the cellular tapetum in dogs. J. Vet. Med. Sci. **76**, 1099–1103.

Zhang, W., Zhang, Y., Kang, L., Gu, X., Wu, H. and Yang, L. (2019): Retinal and choroidal thickness in paediatric patients with hypoalbuminaemia caused by nephrotic syndrome. BMC Ophthalmol. **19**, 44.

Zhao, M., Alonso-Caneiro, D., Lee, R., Cheong, A. M. Y., Yu, W.-Y., Wong, H.-Y. and Lam, A. K. C. (2020): Comparison of choroidal thickness measurements using semiautomated and manual segmentation methods. Optometry Vis. Sci. **97**, 121–127.

Zhu, D., Wang, Y., Zheng, Y. F., Yang, D. Y., Guo, K., Yang, X. R., Jing, X. X., Wong, I. Y., You, Q. S., Tao, Y. and Jonas, J. B. (2017): Choroidal thickness in school children: The Gobi Desert Children Eye Study. PloS One **12**, e0179579.